ALMA MEMO #512
ATMOSPHERIC TRANSPARENCY AT CHAJNANTOR: 1973-2003

Otárola A.[1], Holdaway M.[2], Nyman L-Å.[1], Radford S.J.E.[2], Butler B. J.[3]
[1]European Southern Observatory, Casilla 19001 - Santiago de Chile
[2]National Radio Astronomy Observatory, 949 North Cherry Avenue, 5th Floor, Tucson, AZ 85721
[3]National Radio Astronomy Observatory, 1003 Lopezville Rd., Socorro, NM 87801

Dedicated to our friend and colleague Guillermo Delgado
2005 January

Abstract – Atmospheric conditions at Chajnantor have been monitored since April 1995. Starting then, the National Radio Astronomy Observatory (NRAO), joined by the European Southern Observatory (ESO), Onsala Space Observatory (OSO), and the Nobeyama Radio Observatory (NRO), have operated atmospheric and weather monitoring equipment to characterize the observing conditions for a large radio interferometer for astronomy at millimeter and sub-millimeter wavelengths. The data have demonstrated Chajnantor is an exceptionally good site.

In this work, we examine the atmospheric transparency at Chajnantor before direct measurements begun. We first show the surface water vapor pressure at Chajnantor is a good estimator of the daily-average atmospheric transparency by direct correlation with measurements of optical depth at 225 GHz. Next, we show the surface water vapor pressure at the Calama airport correlates reasonably well with the surface weather conditions at Chajnantor. These findings then allow us to examine the transparency at Chajnantor since 1973 through the analysis of the Calama surface weather data.

Besides, we also include here a determination of the strength of the so-called *Bolivian* winter (regional monsoon) based on a normalized index calculated out of surface water vapour pressure. This index helps us to get the annual regional humidity trend, and in turn can be useful to compare the atmospheric observing conditions from year to year.

1. Introduction

Chajnantor is located just north of the Tropic of Capricorn at latitude South 23°01' and West longitude 67°45' (Figure 18). This site is at 5000 m a.m.s.l on the upper edge of the western slope of the Andes Mountains. The high altitude and the desert climate mean the atmosphere above the site is very dry. This minimizes the absorption of cosmic electromagnetic radiation by water vapor.

This site has been intensively studied to understand its suitability for a large radio interferometer to operate at millimeter and sub-millimeter wavelengths. Measurements with a 225 GHz tipping radiometer [1,2] since April 1995 have demonstrated the good atmospheric transparency at Chajnantor. Further measurements with 183 GHz water vapor radiometers [3,4] have confirmed the dryness of the atmosphere. For April 1995 through August 2003, the median 225 GHz optical depth is 6% (Figure 1) [5]. These data demonstrate the transparency at Chajnantor is among the best in the world for sub-millimeter astronomy [6].

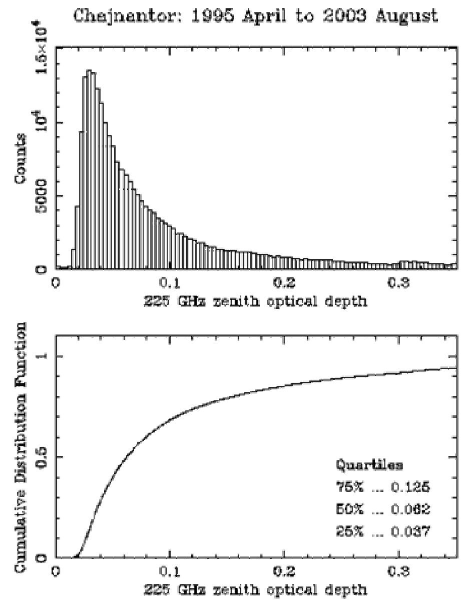

Figure 1 Distribution of 225 GHz optical depth.

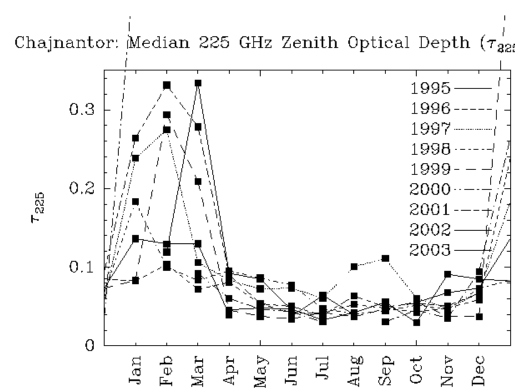

Figure 2 Monthly median 225 GHz optical depth.

From April through November each year, the atmospheric transparency is consistently excellent (Figure 2) [5]. During the summer (mid-December to mid-March), however, there is a well know shift in the regional weather pattern [7]. Then the optical depth is generally higher than in the winter with a noticeable inter-annual variation.

Annual quartiles of the 225 GHz optical depth (Table 1 and Figure 3) were calculated using all available data. Overall, the instrument has operated 77% of the time since April 1995. Instrument malfunctions in 2000 and 2002 caused, unfortunately, particularly large data losses. The overall mean quartiles were computed by weighting the annual statistics by the amount of available data in each year.

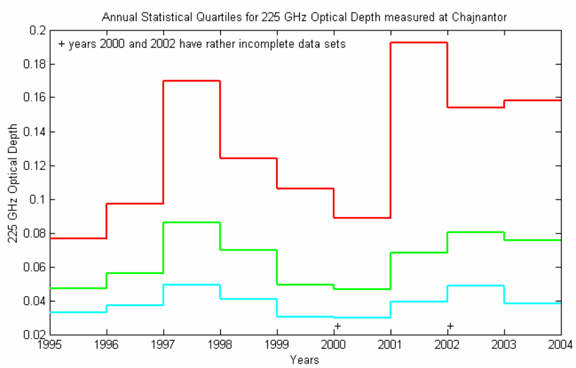

Figure 3 Annual quartiles of the 225 GHz optical depth at Chajnantor.

In this work, we aim to extend our understanding of atmospheric conditions at Chajnantor to the period before we began direct measurements. We first demonstrate the absolute humidity computed from surface measurements is a reasonably good estimator of the daily average atmospheric transparency at Chajnantor. Then we show that weather conditions at Chajnantor can be estimated from surface weather measurements at Calama, 180 km northwest. Finally, we use the historical record of measurements at Calama to characterize the atmospheric transparency condition at Chajnantor for 1973-2003.

2. Data Analysis

2.1. Surface weather data and 225 GHz optical depth at Chajnantor.

For this analysis we considered the surface weather and the 225 GHz optical depth measured at Chajnantor in 1999, both have good coverage with only a gap of about two weeks in March.

Table 1: Annual quartiles of 225 GHz optical depth

Year	1st Quartile	2nd Quartile	3rd Quartile	Total measurements
1995[1]	0.033	0.0475	0.0765	19225
1996	0.0370	0.0562	0.0973	36815
1997	0.0491	0.0861	0.1698	32933
1998	0.0406	0.0695	0.1241	31373
1999	0.0305	0.0492	0.1059	35670
2000[2]	0.0296	0.0465	0.0889	20750
2001	0.0394	0.0684	0.1924	35969
2002[3]	0.0485	0.0802	0.1541	13617
2003[4]	0.0379	0.0757	0.1579	16767

Table 2: Weighted mean quartiles of 225 GHz optical depth, April 1995 through December 1999

Quartile	Weighted mean 04/1995-12/1999
1st	0.0383
2nd	0.0625
3rd	0.1174

The weather station (Figure 4) is located about 30 meters west of the site test containers at Chajnantor. It stores the measurements for the parameters shown in Table 3 as hourly averages. The setup, operations and regular analysis of the data gathered by this weather station are the responsibility of the European Site Characterization Team. Figure 5 shows an example of the air temperature and relative humidity during the first week of January 1999.

The 225 GHz optical depth was measured by a tipping radiometer installed and operated by NRAO. This instrument (Figure 6) is installed so its primary mirror tips from the zenith down to 3 air masses towards the eastern horizon. The instrument makes one tipping scan every 10 minutes and the optical depth is computed from the change of sky brightness temperature with zenith angle. Every 3.5 hours tipping scans are interrupted for measurements of fluctuations in the zenith brightness temperature over one hour [8].

[1] Data available April - December
[2] 109 days data not available
[3] 180 days data not available
[4] Data available January - August

Table 3: Weather station sensors and accuracy

Sensor	Range	Accuracy
Temperature	-30°C - +70°C	0.2°C
Relative Humidity	5% - 95%	1.5%
Barometric Pressure	500 – 800 mbar	+/- 5 mbar
Wind Speed	0 – 200 km/h	0.5 m/s
Wind Direction	0 – 360 deg	3.0 deg
Solar Flux	0 – 1000 W/m^2	

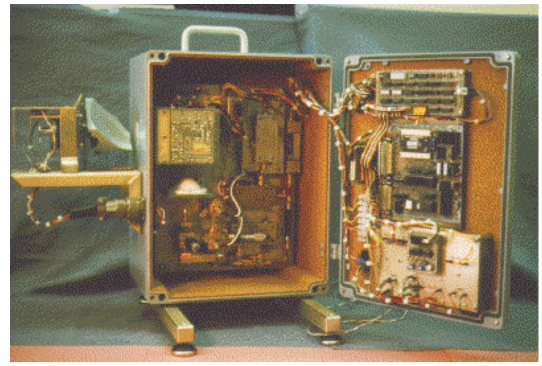

Figure 6 225 GHz tipping radiometer.

Figure 4 ESO Weather Station.

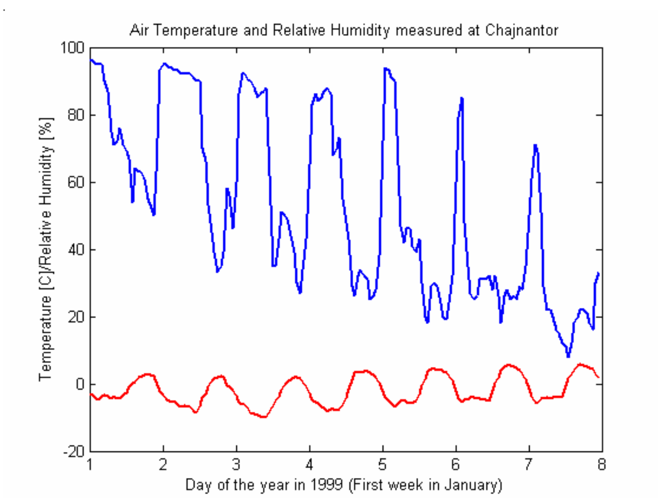

Figure 5 Example of air temperature (lower) and relative humidity (upper) measured at the ESO weather Station.

Figure 7 shows an example of the 225 GHz optical depth during one week in July 1999.

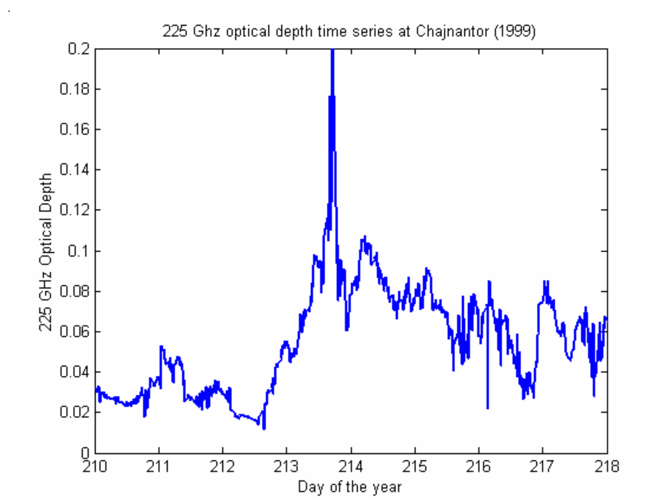

Figure 7 Example of a 225 GHz optical depth time series.

2.2. Correlation between water vapor pressure (wvp) and 225 GHz optical depth at Chajnantor.

The surface air temperature (T) and relative humidity (U) were used to compute the water vapor pressure. We used Magnus Teten's Formula [9] (Equation 1) to determine the saturation water vapor pressure (e_s) and calculated the water vapor pressure (*wvp*) from (Equation 2).

$$e_s = 6.1078\, e^{\left[\frac{17.2694\, T[°C]}{T[°C]+237.36}\right]} \quad [\text{mbar}] \quad (1)$$

$$wvp = \frac{U}{100} e_s \quad [\text{mbar}] \quad (2)$$

We correlated the daily average absolute humidity, represented by the water vapor pressure (*wvp*), with the 225 GHz optical depth (Figure 8). Considering the statistical nature of this study, we correlated the daily averages because the measurement sampling times are different, every 10 minutes for the 225 GHz tipper and every hour for the weather station. The correlation coefficient, R^2=0.75, indicates a significant correlation and the linear regression (Equation 3) establishes the scaling between water vapor pressure (*wvp*) in mbars and the 225 GHz optical depth (τ_{225}).

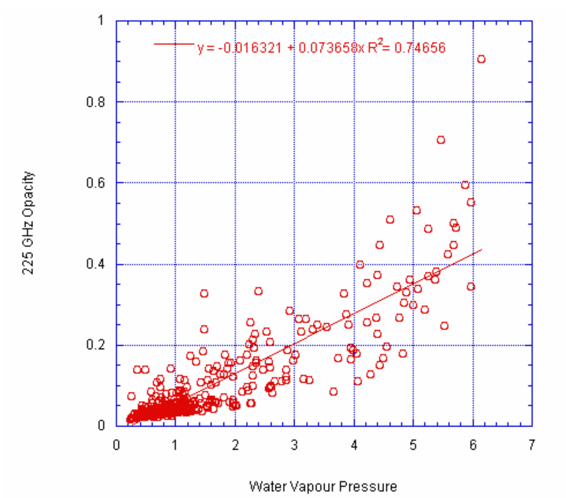

Figure 8 Correlation between water vapor pressure and 225 GHz optical depth at Chajnantor in 1999.

$$\tau_{225} = wvp_{[\text{mbar}]} * 0.0737 - 0.0163 \quad (3)$$

A similar correspondence between surface water vapor pressure and optical depth was observed from measurements made by the Nobeyama Radio Observatory at Rio Frio [10].

We noticed the correlation is weaker when using more frequently sampled data. There are moments when the absolute humidity and optical depth correlate very well and other times when the correlation is quite poor. This might be related to the presence or absence of a temperature inversion layer [10].

For confirmation, we plot together the measured 225 GHz optical depth and the scaled absolute humidity (Figure 9). As to be expected from the significance of the correlation factor, this shows a very good agreement in the trend. Hence, we conclude the surface absolute humidity can be used as a good indicator of the atmospheric transparency at Chajnantor for the given time-scale of daily averages.

2.3. Correlation of surface weather data at Calama and Chajnantor.

The city of Calama is about 180 km northwest of Chajnantor at 2250 m a.m.s.l. (Figure 18). The Domeyko mountains, with peaks as high as 4500 m, lie between Calama and Chajnantor. Both Calama and Chajnantor are east of the costal mountains. Because of a persistent offshore temperature inversion layer and a high pressure anticyclone, the humidity present at the ocean-atmosphere boundary remains trapped west of the costal mountains. This explains, in part, the extreme aridity of the Atacama Desert. Furthermore, the atmospheric water vapor content decreases with altitude, so Chajnantor is even drier than Calama.

ESO arranged with the Chilean National Weather Office[5] to obtain the surface weather data series gathered at the Calama airport for 27 years, August 1973 through December 2000. The air temperature, relative humidity, barometric pressure, and wind speed and direction were recorded at 12, 15, 18, 21, and 24 hours of UT following the established protocol. Unfortunately, we have found the wind speed and wind directions are gross estimations of the real conditions and they can not be use for the determination of advection of humid air mass from the Calama area into the Chajnantor site.

Daily averages were computed from these measurements. Because the measurement period covers roughly sunrise to sunset, these averages represent daytime conditions rather than true 24h averages. In principle, we could adjust the measurements to better represent the true 24h conditions, but we have elected not to make any adjustment. At Chajnantor, the diurnal transparency variations are small during the winter and modest during the summer. Hence, we expect the daytime measurements from Calama will still be representative of the overall atmospheric conditions.

Figure 10 shows the daily averages of water vapor pressure at Calama plotted against the water vapor pressure at Chajnantor. The straight line over the data points correspond to the regression function (Equation 4) which best fits the data. The correlation coefficient, R^2=0.55, which is an indication surface weather conditions in Calama and Chajnantor are correlated to a reasonably good level.

[5] Oficina Meteorológica de Chile

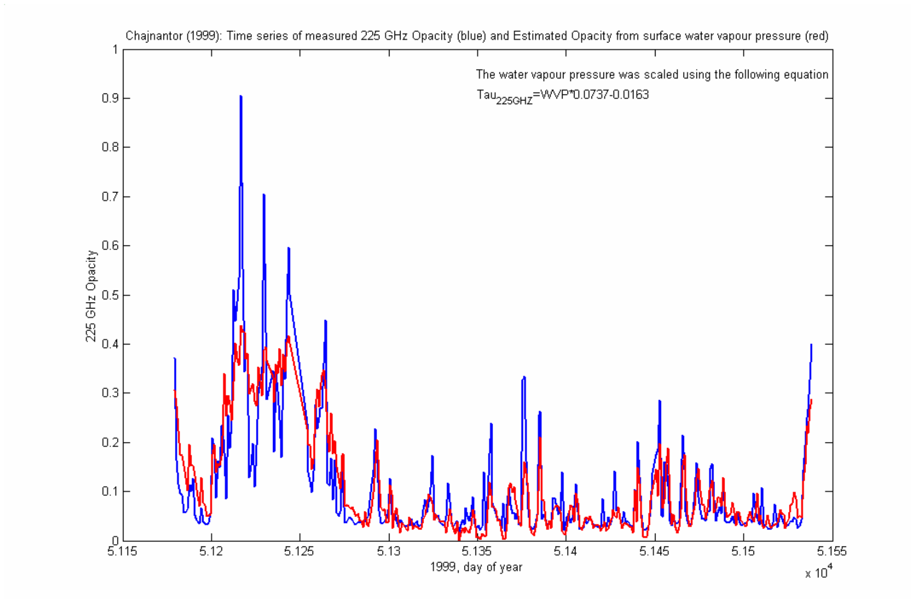

Figure 9 225 GHz data series, Cyan (measured daily averages), Red (water vapor pressure scaled using the correlation in equation 3).

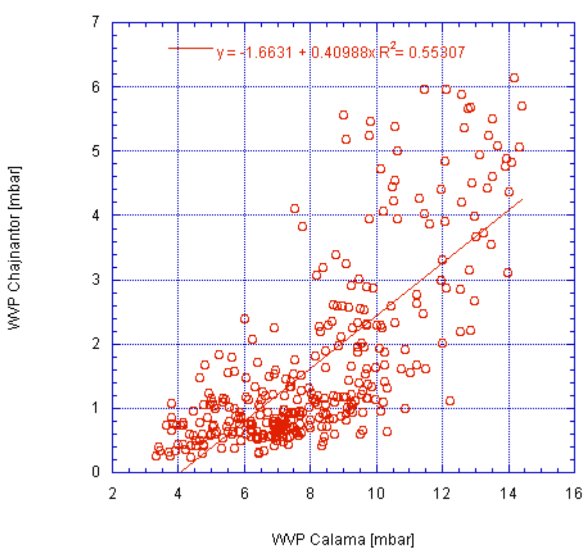

Figure 10 Daily average water vapor pressure at Calama and at Chajnantor, 1999.

$$wvp_{CHAJ} = wvp_{CAL}[\text{mbar}] \times 0.41 - 1.66 \quad [\text{mbar}] \quad (4)$$

Even though the linear regression shows a relatively good correlation between Calama and Chajnantor, the actual situation is more complicated. Water vapor decreases exponentially with altitude (Equation 5) and water vapor measurements obtained at different altitudes in the troposphere (Δh=2.75[6] km) are correlated by mean of the water vapor scale height factor (h_0). This factor is not constant and changes following the atmospheric conditions, this explains the dispersion we see in Figure 10. More difficult to explain is the offset we see in the regression of Equation 4. This offset might have origin in some calibration issues affecting the weather sensors, specifically, the temperature or relative humidity sensors in the weather stations where the datasets have been gathered.

The literature indicates a nominal value of 1.8 km for h_0. Independent analysis by Butler [11] and Otárola [12] of atmospheric profiles measured from radiosonde launches from the Chajnantor site, indicate the mean value for h_0, for the atmosphere above the Chajnantor site, is 1.4 km and the 3rd quartile is 1.75 km.

$$wvp_{CHAJ} = wvp_{CAL} \times e^{-\frac{\Delta h}{h_0}} \quad [\text{mbar}] \quad (5)$$

[6] Altitude difference between Calama and Chajnantor in km.

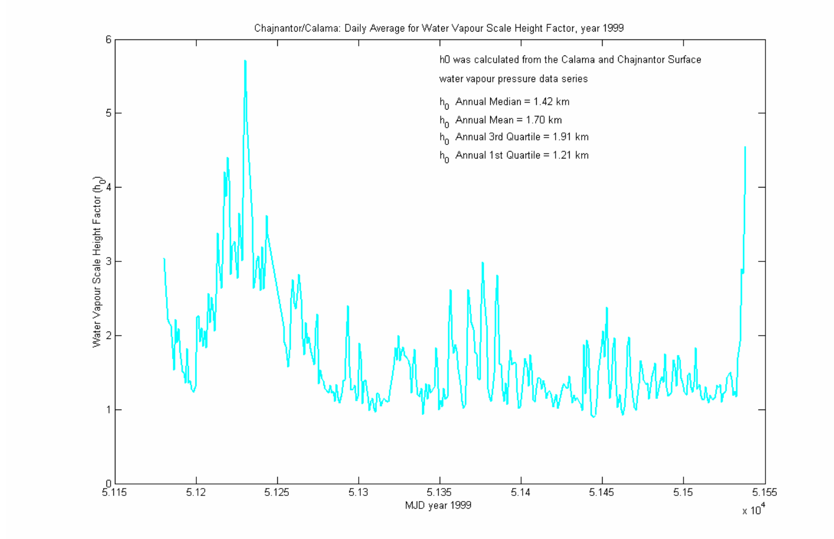

Figure 11 Time series of h_0^* determined from the Calama and Chajnantor water vapor pressure data, 1999.

As stated above, the scaling factor between conditions at Calama and at Chajnantor varies from day to day. Because of the distance between the two places (180 km), this scaling will not necessarily correspond to the real "water vapour scale height". We denote the Calama/Chajnantor scaling factor h_0^*.

Figure 11 shows the time series of the scaling factor obtained by using the 1999 Calama and Chajnantor sets of absolute humidity.

From this figure we can easily notice what we already have mentioned earlier, that this scaling factor changes from day to day following the particular atmospheric conditions. Since the trend looks similar to the 225 GHz opacity (Figure 9), we calculated the correlation between the scaling factor and the 225 optical depth at Chajnantor. The linear regression (Equation 6) has a correlation coefficient of R^2=0.67, indicating a quite good correlation between the Calama-Chajnantor absolute humidity scaling factor and the atmospheric transparency at Chajnantor. These two results, the good correlations shown in Equations 4 and 6, validate the use of the Calama data for a retrospective view of the atmospheric conditions at Chajnantor.

$$\tau_{225\mathrm{GHz}} = 0.13 * h^*_{0[\mathrm{km}]} - .12 \qquad (6)$$

For scaling the Calama surface absolute humidity data to the altitude of Chajnantor we decided to look for the water vapor scaling factors that better reproduce the statistics (quartiles) of the atmospheric conditions based in the data we have gathered for Chajnantor in the period 1995 through 2000 (Table 2). Using different scaling factors to convert all the Calama data (1973-2000) to the altitude of Chajnantor will help us not only to get the statistical trends for the atmospheric transparency at Chajnantor, but also the absolute values for the statistics (in terms of quartiles) will come close to measured values for these quartiles.

Table 4 225 GHz opacity statistics reproduced using Calama surface weather data as starting point.

Statistics	1st quartile	2nd quartile	3rd quartile
τ_{225} (Measured at Chajnantor)	0.0383	0.0625	0.1174
τ_{225} (Reproduced using Calama data)	0.0384 h_0=1.52 km	0.0628 h_0=1.56 km	0.1173 h_0=1.84 km

Figure 12 shows the opacity data series measured at Chajnantor during April 1995 through December 1999 together with the opacity estimated from Calama surface data with Equation 7 and the average of the scale factors in Table 4 (h_0^* average = 1.64 km). The 225 GHz opacity estimated from the Calama surface data follows the mean trend for the measured 225 GHz opacity very well but fails to reproduce the very opaque atmospheric conditions. A zoom of this plot is available in Figure 13.

A possible explanation is that water vapor is roughly exponentially distributed, but the scale height is larger during bad conditions as we can infer from the regression in Equation 6. On the other hand, as we can derive from this plot, during the part of the year not affected by the monsoon the absolute correspondence between the two trends improves. We shall keep in mind that we are talking about daily average conditions.

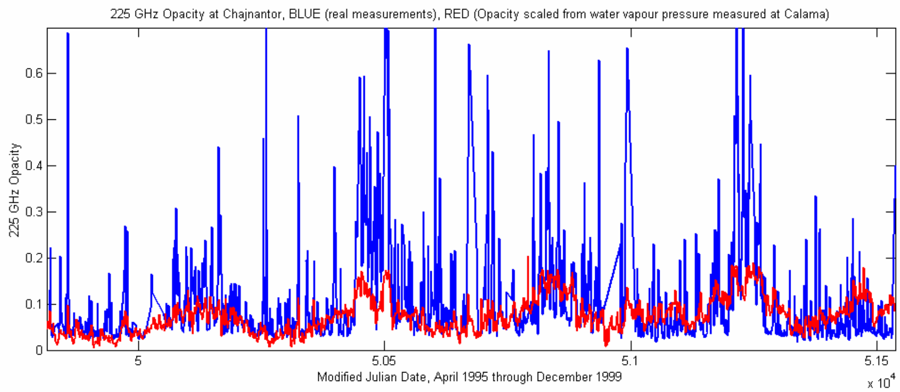

Figure 12 225 GHz optical depth data series, measured data in blue and scaled data using h_0=1.64 km in red.

Considering we have been able to reproduce several parameters from the Calama data for those years when we have information available at both sites, Calama and Chajnantor, we will proceed now to get a statistical view of the atmospheric transparency at Chajnantor prior to the installation of monitoring and atmospheric sounding equipment.

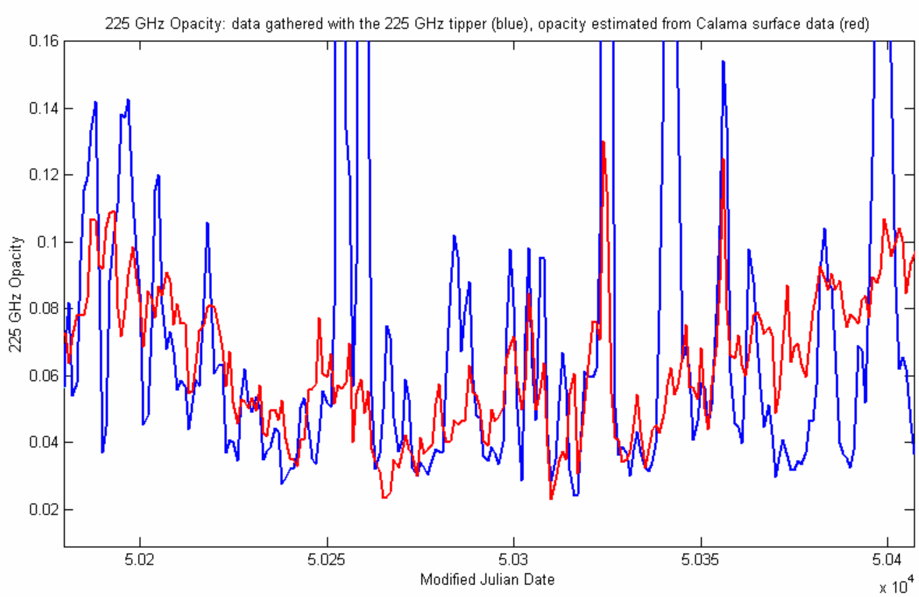

Figure 13 225 GHz optical depth (Zoom from Figure 12).

2.4. Retrospective view of the atmospheric transparency at Chajnantor during 1973 through 2003.

The annual quartiles of the Calama water vapor pressure for 1973-1998 were scaled with the h_0^* factors in Table 4 and with Equation 7 to estimate the atmospheric transparency at Chajnantor (Δh=2.75 km).

$$\tau_{225GHz} = 0.0737 \times wvp_{CAL} \times e^{-\frac{\Delta h}{h_0}} - 0.0163 \quad (7)$$

The resulting historical record (Figure 14) shows Chajnantor has enjoyed excellent atmospheric transparency throughout the past 30 years. This result supports similar conclusion based on analysis of a large scale regional climate database [13]. For comparison, the annual optical depth statistics obtained from direct measurements are shown together with the statistics obtained from the scaled Calama data. During the overlap, 1995 through 1998, the date shows good agreement. In 1997, however, the Calama data indicated better conditions than were actually observed at Chajnantor.

However, what we are really interested in here is the general trend. Figure 14 shows that the overall conditions at Chajnantor have remained stable since 1973. The overall baseline through the statistics shows no long term trend. There are, however, noticeable inter-annual variations. These may be related to the occurrence and strength of the regional monsoon (the so-called Bolivian Winter).

Is interesting to note peaks in the inter-annual variations in 1982-1983, 1990-1991, and 1997-1998 (as seen in Figure 14) also match the years when El Niño weather patterns were recorded. Of these three periods, the El Niño events were especially strong in 1982 and 1997 [14]. If this correlation is true, then we should expect larger opacities at Chajnantor during El Niño conditions. Since atmospheric scientists are monitoring the ocean temperature as a way to anticipate the occurrence of an El Niño event, we might well use that information to plan or constrain the observing schedule.

For completeness, we calculated the power spectrum of the Calama surface water vapor pressure over 27 years (Figure 15). The annual variation peak, corresponding to the summer shift in the regional weather pattern is evident.

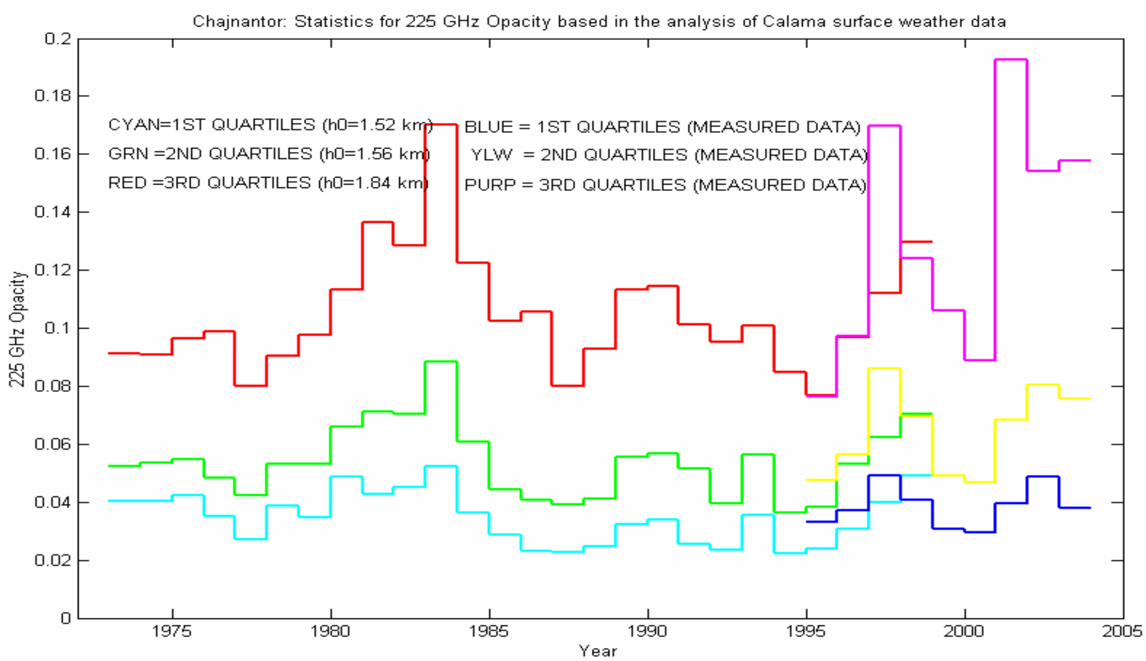

Figure 14 Historical view of atmospheric transparency at Chajnantor (1973-2003).

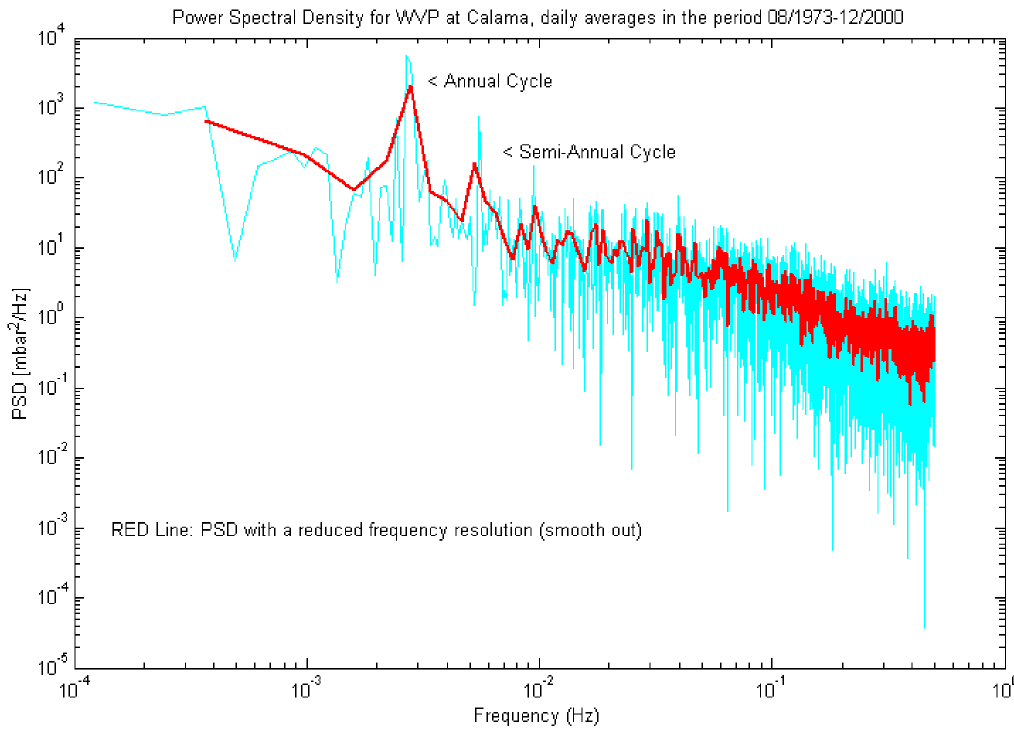

Figure 15 Power Spectrum for the WVP at Calama.

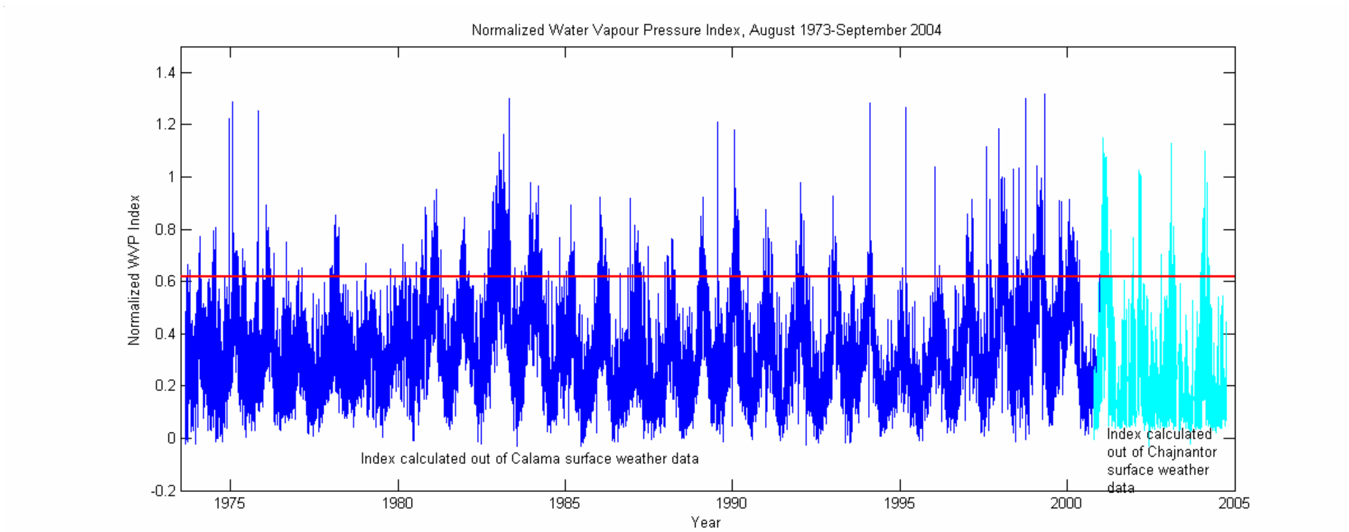

Figure 16 Normalized Water Vapour Pressure Index (NWVPI) and threshold value of 0.618.

Since the inter-annual variations are probably due to variations in the strength of the regional monsoon, we decided to follow the approach suggested by Zeng and Lu [15], in the determination of the monsoon onset and retreat dates by mean of calculating a Normalized Water Vapour Pressure Index similar to their Normalized Precipitable Water Index (NPWI).

Zeng and Lu provided empirical evidence to prove that the monsoon onset and retreat can be estimated by comparing the daily average NPWI against a threshold value of 0.618. This novel metric was found to consistent with existing monsoon information and has been proposed as a way to refine the definition of monsoon regions on a grid-cell by grid-cell basis around the globe [15].

$$\mathrm{NWVPI} = \frac{\mathrm{wvp} - \mathrm{wvp}_{\mathrm{min}}}{\mathrm{wvp}_{\mathrm{max}} - \mathrm{wvp}_{\mathrm{min}}} \qquad (8)$$

Equation 8 shows the expression we have used for the normalized water vapour pressure index (NWVPI) where WVP_{max} and WVP_{min} are the average of the annual water vapour pressure maxima and minima, respectively. Figure 16 shows the index as determined from Equation 8 and using the Calama surface weather data for the period 1973-2000 and the Chajnantor data for the period 2000-2004. For Chajnantor, the NWVPI index was obtain using values of WVP_{max} and WVP_{min} calculated out of the four years of Chajnantor data. The periods of time when the index is definitely above the threshold value (0.618) is an indication of that the regional monsoon is taking place. The monsoon itself is characterized by a reversal of the wind direction [16], and a higher humidity and rainfall phase [15]. Therefore, we can use the fraction of the year the Normalized Water Vapour Pressure Index is above the threshold value of 0.618 to compare how much or less humid has been the atmosphere from year to year at Chajnantor (see Figure 17). The arrow in Figure 17 shows the year we started the site testing activities.

3. Conclusions

Surface weather data from the Calama airport for 1973 through 2000 were obtained by ESO from the Chilean National Weather Office. These data were analyzed together with 225 GHz optical depth and surface weather measurements at Chajnantor.

We find the surface water vapor pressure at Chajnantor is a reasonable good predictor of the daily average atmospheric transparency (§ 2.2). We also find the daily average surface water vapor pressures at Calama and Chajnantor show a reasonable correlation for this study (§ 2.3). Hence, the Calama surface measurements can be used as an indicator of the atmospheric transparency at Chajnantor.

We have also found a correlation between the water vapour scale height factor and the atmospheric optical depth at 225 GHz (regression in Equation 6). This is reasonable under the assumption water vapour, at daily average level, distributes exponentially with altitude and there is no significantly large amounts of water vapour trapped at any layer higher in the atmosphere. The water vapour scale height can be derived from surface weather data gathered at two stations located at different elevations. Therefore, we can monitor this parameter by having weather stations installed at the Operations Support Facility and the Array Observatory Site, at 2800 m and 5050 m elevation, respectively.

We then applied these correlations to the historical record (§ 2.4). Although, there are inter-annual variations, the excellent atmospheric transparency at Chajnantor has persisted over the past 30 years. The inter-annual variations are attributed to the variability in the strength of the regional monsoon, so-called the *Bolivian* Winter.

Figure 17 shows that from 1973 through 2005 the site has experienced two periods of noticeable higher atmospheric humidity, probably associated with the occurrence of El Niño Event. This information is also confirmed by our estimations of the atmospheric optical depth quartiles as seen in Figure 14.

Acknowledgement

The weather database from Calama was acquired by ESO under Work Package WP391 in year 2000, and with the support of the WP Manager Daniel Hofstadt.

We also thank Dr. Xubin Zeng, Professor at the atmospheric Sciences Institute, University of Arizona, for his comments on the determination of the normalized water vapour pressure index from surface weather data.

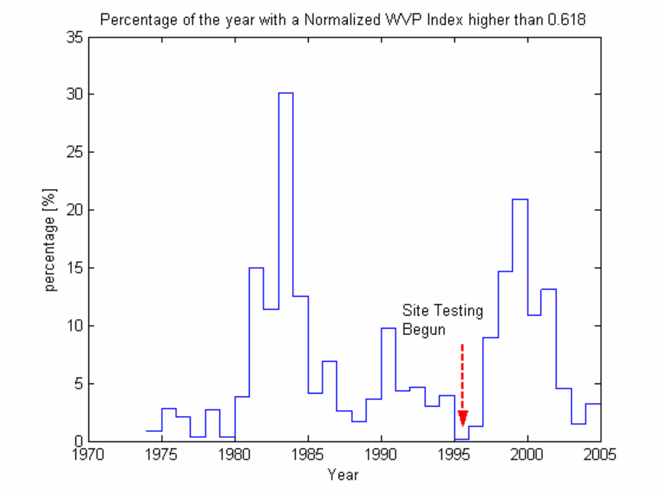

Figure 17 Percentage of the year with a Normalized Water Vapour.

Bibliography

Alma Memo Series available at: http://www.alma.nrao.edu/memos/

[1] McKinnon, Measurement of Atmospheric Opacity Due to Water Vapor at 225 GHz, MMA Memo #40, June 1987.

[2] Liu Z-Y, 225 GHz Atmospheric Receiver – User's Manual, MMA Memo #41, August 1987.

[3] Hills R., Gibson,H., Richert J., et. al., Design and Development of 183 GHz Water Vapor Radiometers, ALMA Memo #352, March 2001.

[4] Delgado G., Otárola A., Belitsky V., Urbain, D., Hills, R., Martín-Cocher, P., The Determination of Precipitable Water Vapor at Llano de Chajnantor from Observations of the 183 GHz Water Line, ALMA Memo #271.1, October 1999.

[5] Radford S.J.E., ALMA Site Studies Internet Site, http://www.tuc.nrao.edu/alma/sites/Chajnantor/data.c.html

[6] Radford S.J.E., Chamberlin R.A., Atmospheric Transparency at 225 GHz over Chajnantor, Mauna Kea, and the South Pole, ALMA Memo #334-1, December 2000.

[7] Bustos., R., Summer Climate over Chajnantor, ALMA Memo #379, July 2001.

[8] McKinnon, M., Measurement of Atmospheric Phase Stability with a 225 GHz Radiometer, MMA Memo #49, May 1988.

[9] Murray, F.W., On the computation of saturation vapor pressure, L. Appl. Meteorol., 6, 203-204, 1967.

[10] Holdaway, M., Ishiguro, M., Nakai, N., Matsushita, S., Correlation between Opacity and Surface Water Vapor Pressure Measurements at Rio Frio, ALMA Memo #158, August 1996.

[11] Butler., B. et. al., Radiosonde Measurements at Chajnantor, in preparation.

[12] A. Otárola, Determination of the Water Vapor Scale Height Factor for the Atmosphere above the Chajnantor Site, ESO Internal Document, July 1999, available from the author (aotarola@eso.org).

[13] R. Bustos, G. Delgado, L-Å Nyman, S. Radford, 52 Years of Climatological Data for the Chajnantor Area, ALMA Memo #333, August 2002.

[14] NOAA Web site, Multivariate ENSO Index, http://www.cdc.noaa.gov/ENSO/enso.mei_index.html

15] Xubin Zeng, Er Lu, Globally Unified Monsoon Onset and Retreat Indexes, Notes and Correspondence, American Meteorological Society, June 2004.

[16] Warren, B. A., Ancient and Medieval Records of the Monsoon Winds and Currents of the Indian Ocean, J. S. Fein and P. L. Stephens, Eds., John Wiley & Sons, 3-32, 1987.

Figure 18 Courtesy of Turistel S.A. http://www.turistel.com.